

Seismicity Study of Bandar-e-Anzali Area by Zoning Peak Ground Acceleration and Response Spectra

Reza Jamshidi Chenari^{1*}, Saeid Pourzeynali¹, Behrooz Alizadeh²

¹Associate Professor, Department of Civil Engineering, Faculty of Engineering, University of Guilan, Rasht, Gilan Province, Iran

²M.Sc Graduate, Department of Civil Engineering, Faculty of Engineering, University of Guilan, Rasht, Gilan Province, Iran

*Corresponding author: Reza Jamshidi Chenari

| Received: 10.02.2019 | Accepted: 21.02.2019 | Published: 23.02.2019

DOI: [10.21276/sjce.2019.3.1.1](https://doi.org/10.21276/sjce.2019.3.1.1)

Abstract

Bandar-e-Anzali is located among many active faults in Guilan Province in the north of Iran, and seismologically is one of the active regions of Iran. Numerous severe historical and instrumental earthquakes, including three earthquakes with magnitude more than 7 in this region, can be an evidence of this claim. The objective of this paper is to estimate acceleration coefficient for different levels of seismic activities within the city surrounding area. For this purpose, a list of major faults, as well as the reported historical and instrumental earthquakes occurred within a radius of 200 km around the area, till 2013 A.D. are collected. In this paper, after culling and removing aftershocks and foreshocks, first the Poisson behavior of the remaining earthquakes is studied; and then by calculating the frequency of earthquakes and using universal probabilistic relationships, the seismicity parameters of this region is obtained. Finally, the site-specific response spectra and the peak ground acceleration coefficients for this city and suburbs are obtained using SeisRisk III hazard analysis program. The results of this study show that the active seismicity in the south area of this city is much more than its northern parts.

Keywords: Earthquake occurrence; Peak Ground Acceleration; Response Spectrum; Attenuation Relationship; Bandar-e-Anzali

Copyright © 2019: This is an open-access article distributed under the terms of the Creative Commons Attribution license which permits unrestricted use, distribution, and reproduction in any medium for non-commercial use (NonCommercial, or CC-BY-NC) provided the original author and source are credited.

INTRODUCTION

Bandar-e-Anzali is located in the geographic range of 49.22°-49.36° east longitude and 37.20°-37.26° north latitude; in the Sefidrud delta and western domain of Alborz mountain range, with an area of 275 square kilometers. In terms of topography, this city is placed on a smooth and extremely lowland region that does not exceed 4 meters above Caspian Sea level. Also, this city is placed nearly 23 meters below the surface waters of the world. Due to the dense population, and existing important structures such as jetties of Bandar-e-Anzali, seismicity studies of the area are deemed to be crucially important. Considering the severe historical and instrumental earthquakes in the region including Manjil-Rudbar great earthquake of 1990, high intensity earthquakes are always highly probable to occur in the region.

The main objective of this paper is to evaluate the base acceleration coefficient for Bandar-e-Anzali area, introduced in the local and domestic Iranian seismic code by adoption of different possible methods. For this purpose, the latest status of the major faults in the area [1-7], reported historical earthquakes [8] and registered instrumental earthquakes till 2013 A.D.,

within a radius of 200 km from the center of the city have been collected and studied.

In the present study, after culling and removal of aftershocks and foreshocks from the earthquake catalogue of the region by using space-time windows method [9], the Poissonian behavior of the occurred earthquakes is studied. Seismicity parameters of the region are then obtained by calculating the frequency of earthquakes and performing seismic hazard analysis using the probabilistic relationships of Kijko *et al.*, [10-12]. Finally, the site-specific response spectra and zoning peak ground acceleration coefficient for Bandar-e-Anzali and suburbs have been proposed, using SeisRisk III earthquake hazards program.

Seismicity and Seismotectonics of Bandar-e-Anzali Area

Generally, in seismotectonics viewpoint, Iran area can be divided into four states: strip folded-driven Zagros, Makran region in southeast of Iran, the Central Iranian plateau, and Alborz mountain range. In terms of seismotectonics, existing multiple faults in the Alborz region have led to the recognition of this region as one of the most seismic regions of Iran with high seismic risk. More than 24 major and minor faults have been

identified in regions surrounding Guilan province [1-7]. Finally, by considering various factors, including the proximity to Bandar-e-Anzali and fault's seismicity background, 16 faults are chosen for seismicity studies

in this area. Figure-1 shows the last state of these seismicity resources in areas surrounding Bandar-e-Anzali.

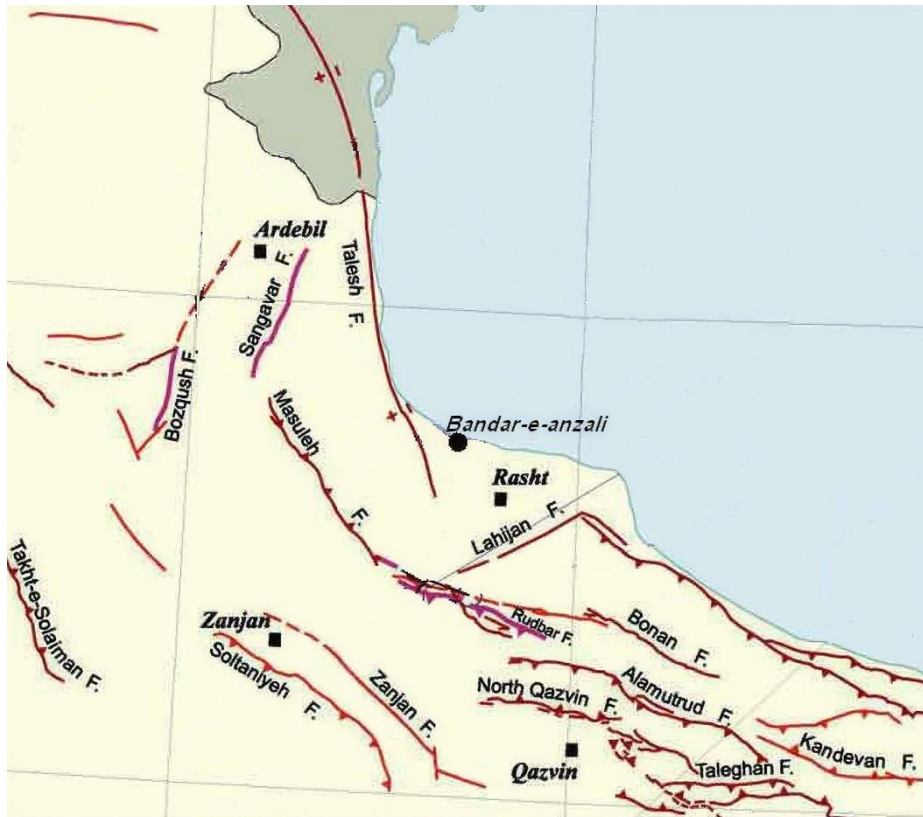


Fig-1: Active fault distribution in Bandar-e-Anzali area

More descriptions of active faults in this area are provided in Table 1. It should be noted that there are many different relationships between the maximum

earthquake magnitude and the rupture length of the source fault in terms of different magnitude scales.

Table-1: Profile of main active faults within a radius of 200 Km around Bandar-e-Anzali

No.	Fault name	Mechanism of fault	Overall length of fault (km)	Rupture length of fault (km)	Background seismicity	Maximum earthquake magnitude (M_S)
1	Alborz (Caspian)	Reverse Thrust	523	160	7	7.7
2	North Alborz	Reverse Thrust	360	110	4	7.5
3	Astara (Talesh)	Reverse Thrust	400	120	2	7.6
4	Alamutrud	Reverse Thrust	140	70	3	7.3
5	Rudbar	Right Lateral	93	47	2	7
6	Soltanieh	Reverse Thrust	140	70	1	7.3
7	Taleghān	Reverse Thrust	64	32	2	6.8
8	Lahijan	Reverse Thrust	92	46	-	7
9	Masouleh	Reverse Thrust	90	45	-	7
10	Sangavar	-	61	31	-	6.8
11	Bozqush	Reverse Thrust	70	35	1	6.9
12	Banan	-	74	37	1	6.9
13	Zanzan	-	137	69	-	7.3
14	North Qazvin	Reverse Thrust	60	30	1	6.8
15	Javaherdasht	Reverse Thrust	74	37	-	6.9
16	Zardgoli	Reverse Thrust	40	20	-	6.6

In this paper, the relationship proposed by Nowroozi [13] has been used in terms of surface-wave magnitude scale (M_S) and effective rupture length of the fault of Iran as follows:

$$M_S = 1.259 + 1.24 \log(L) \quad (1)$$

Where L is the effective rupture length of the fault, expressed as a fraction of the overall length of the fault. Reviewing the history of the Alborz seismicity reveals that the occurrence of numerous devastating historical and instrumental earthquakes in this region of country has led to the destruction of many towns and

villages. In Table-2, some of these destructive earthquakes are shown. Note that in relative seismic hazard zonation of Iran, Bandar-e-Anzali region is marked as high relative risk area.

Earthquake Catalog

To obtain the seismicity parameters and perform seismic hazard analysis, 17 historical reported earthquakes and more than 260 instrumental recorded earthquakes with magnitudes greater than 4 on surface-wave magnitude scale (M_S) to the end of 2013 A.D. are collected in the surrounding area of Guilan.

Table-2: Historical and instrumental strong earthquakes occurred within a radius of 200 km around Bandar-e-Anzali area

No.	Year of earthquake occurrence	Place of earthquake occurrence	Magnitude (M_S)
1	958	North Karaj	7.7
2	1177	East Mahdasht	7.2
3	1485	Deilam, South Ramsar	7.2
4	1608	Taleghan	7.6
5	1844	East Mianeh	6.9
6	1879	Bozqush	6.7
7	1896	Khalkhal	6.7
8	1924	East Garmi	8.2
9	1960	Southern Shaft (Manjil)	6.5
10	1962	Boein Zahra	7.2
11	1978	Northeast Hashtpar (Caspian Sea)	6.9
12	1990	Southern Shaft (Manjil)	7.4
13	1997	Nir, Ardebil Province	6.1
14	2002	North Razan	6.7
15	2005	Mianeh	4.6
16	2008	East Zanjan	4.8

All the instrumental earthquakes recorded in Iran since 2004, on the one hand, and earthquakes with magnitudes larger than 3.5 on surface-wave scale (M_S) from 2004 onwards, on the other hand, are considered

in the analysis. Figure-2 shows the distribution of instrumental earthquakes of the catalog till 2013 A.D. with magnitude greater than 3.5 on surface-wave scale (M_S).

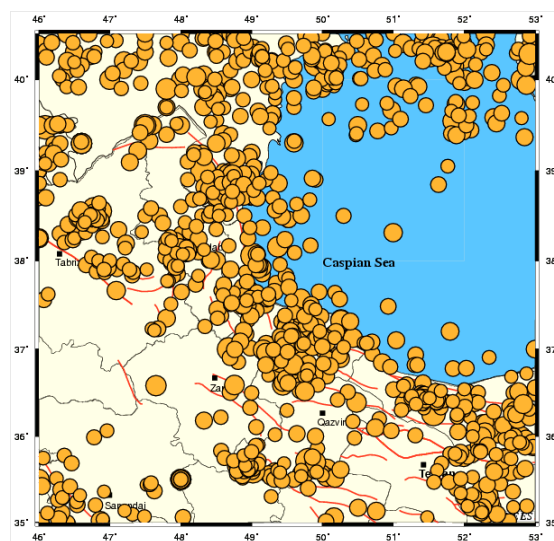


Fig-2: Distribution of instrumental earthquakes in Bandar-e-Anzali zone with magnitude M_S greater than 3.5

For assessment of seismicity activity in any region, all the earthquake magnitudes that are used should be given in a single scale. For this purpose, conversion relationships are required to inter-convert different magnitude scales. Various relationships are proposed for this purpose around the world; however, many of these relationships are developed based on the earthquakes occurred around the world, and these relationships may not provide appropriate results for a specific area, such as Iran.

Nevertheless, some of these relationships are provided based on the earthquakes occurred in Iran, such as the relationships presented by Mirzaei *et al.*, [14], but these relationships do not cover all magnitude scales. Moreover, the data used to develop these correlations are not comprehensive. Several seismic hazard studies are also performed by different researchers including Nowroozi and Ahmadi [15], Tavakoli [16], Amiri *et al.*, [17], Hamzehloo *et al.*, [18] and Zare [19] for the whole country of Iran, and the research studies performed by Amiri *et al.*, [20-22] for the metropolis of Tehran and Guilan province and Moghaddam *et al.*, [23] for Tabriz. However, in all these studies, no new relationship is developed for Iran, and only the previous relationships for other countries, were used. Therefore, in this paper, it has been tried to use the new relationships proposed by Alizadeh *et al.*, [24] to inter-convert the different earthquake magnitude scales for Iran. Considering the vast number of earthquake data covered by this catalog and of course their remarkable accuracy, these new relationships can be adopted for the assessment of seismicity in each favorite part of the area and even the adjacent lands.

Seismicity Parameters of Bandar-e-Anzali

So far, various statistical methods have been provided to estimate the seismicity parameters, which are entirely based on the basic Gutenberg-Richter relationship. Basic method of Gutenberg-Richter establishes a linear relationship between the frequency and magnitude of earthquakes as below:

$$\log \lambda(m) = a - bM \quad (2)$$

Where $\lambda(m)$ is the rate at which the earthquakes with magnitude equal or greater than M occur at a specific time period; b is the seismicity coefficient and a is the number of events greater than M_{\min} . Due to the inadequate and low accuracy of existing data, using the basic Gutenberg-Richter method [25] and curve fitting procedure to obtain the seismic parameters of the region, do not render accurate results. Since these parameters play important role in seismic hazard analysis of any region and return period of the earthquakes, it is attempted to use a more accurate and genuine methodology, compatible with the seismic data in Iran. All methods have been introduced after the preliminary Gutenberg-Richter approach that is established on two earthquake patterns:

- Earthquakes reported in the historical manuscripts before the advent of the seismograph machines that have occurred over a period of a few hundred years.
- Complete instrumental data which are registered in relatively short periods of time.

Indeed, an important issue that should be considered in estimating the parameters of the probability density function for magnitude is the amount of uncertainty and the imperfection embedded in earthquake data. The methods which are mainly used in estimation of the seismic parameters (rate of seismic activity λ and parameter b in Gutenberg-Richter equation) were found unsuitable for imperfect historical data. The most appropriate method for analyzing the historical part of the data catalog is the extreme distributions. The drawback of this method is however, that it cannot be used to analyze instrumental data. Some researchers suggest another method for estimating the seismic activity parameters. This method removes the historical data due to their incompleteness. Thus, the remaining part of the catalog which is called the complete part of the catalog can be used by any standard method to be analyzed. Nonetheless, it is clear that this procedure is not effective, because the quantitative assessment of strong seismic events based on observations over a short period of time is prone to tremendous errors. However, the maximum likelihood estimation method which was used by Kijko [10, 11] for the first time is a good model for assessment of the seismic parameters. This method is based on the two fundamental assumptions:

- The occurrence of earthquakes is independent in time and space.
- The area under investigation is homogeneous in terms of seismic properties.

This method, presented as a computer program for analysis of historical earthquakes, will make use of the double truncated Gutenberg-Richter exponential distribution to analyze the instrumental earthquakes, and finally combines the results of analyses. It is to be noted that the Kijko method has the ability to divide the instrumental part of the catalog to some subcatalogs and considers different threshold magnitude levels for them, individually. Earthquake subcatalogs of the instrumental earthquakes of Iran with threshold levels proposed by Alizadeh *et al.*, [26] were implemented to Kijko method which is based on random occurrence of the earthquakes. Accordingly, the following magnitude threshold levels (MTLs) are introduced:

- For earthquakes recorded by analog devices (1900-1963) (MTL=4.5).
- For recent earthquakes (1964-2003) recorded with higher accuracy than previous earthquakes (MTL=4).
- For new earthquakes (2004-2010) recorded with very good accuracy and frequency (MTL=3.5).

Thus, having in hand appropriate magnitude threshold levels for each of the instrumental earthquake subcatalogs, results are obtained with greater reliability.

According to the above descriptions, the entire available earthquake data catalog for Bandar-e-Anzali area are divided to four subcatalogs including one historical and three instrumental earthquakes given in the following:

- Historical earthquakes (till 1900) with uncertainty 0.4 (Case # 1).
- Earthquakes recorded by analog devices (1900-1963), with uncertainty 0.3 and magnitude threshold $M_s=4.5$ (Case # 2).
- Recent earthquakes (1964-2003) recorded with higher accuracy than previous earthquakes, with uncertainty 0.2 and magnitude threshold $M_s=4$ (Case # 3).
- New earthquakes (2004-2013) recorded with very good accuracy and frequency, with uncertainty 0.1

and magnitude threshold $M_s=3.5$ (Case # 4).

As noted earlier, Kijko method has the ability to evaluate the seismicity parameters individually for each subcatalog of the considered earthquakes, but the best results can be obtained when the combination of all the subcatalogs are considered [12]. The results of seismicity parameters using the above procedure for Bandar-e-Anzali and the surrounding area of radius 200 km are given in Table-3.

From Table-3, it is noteworthy that $\beta = b \ln 10$ where b is the seismicity coefficient (Eq. 2); and $\lambda(m)$ is the annual mean rate of earthquake occurrence. In 1996, Tavakoli also performed a research study to obtain the seismicity parameters for the whole area of Iran, only using the instrumental data recorded in time period 1929-1995, in which the province No. 20 includes the Bandar-e-Anzali area, from which some of the results, for comparison, are given in Table-4.

Table-3: Seismicity parameters obtained by Kijko 2000 computer program for Bandar-e-Anzali

Catalog	Parameter	Value	Data contribution to the parameter (%)			
			Case#1	Case#2	Case#3	Case#4
Only historical data	β	2.12	100	0	0	0
	$\lambda(M_s = 4.5)$	0.48	100	0	0	0
Only instrumental data	β	2.20	0	36.7	40.4	17.8
	$\lambda(M_s = 4.5)$	0.44	0	15.7	51.2	33.0
Combination of historic and instrumental data	β	2.13	33.7	26.1	28.1	12.2
	$\lambda(M_s = 4.5)$	0.46	11.8	13.9	45.1	29.1

Table-4: Seismicity parameters for Guilan Province calculated by Tavakoli [16]

Province No.	Span of Time	β	M_{max}	$\lambda (M_s=4.5)$
20	1929-1995	2.32 ± 0.16	7.5 ± 0.9	0.33

By comparing Tables 3 and 4, it can be seen that the annual mean rate of earthquake occurrence obtained in this paper is higher than the values reported by Tavakoli [16]. The main reason behind this is the number of earthquakes in this paper in comparison to Tavakoli’s studies, as current study considers numerous earthquakes occurred after 1995. The slight deviation between the seismicity coefficients presented in the current study and those of Tavakoli emanates from the historical data which was neglected in Tavakoli’s analysis.

Prediction of Earthquake Occurrence

Various models are presented for prediction of earthquake occurrence, which the most common one is the Poisson model. In the Poisson distribution it is assumed that the earthquake data are independent of time. Poisson model can be expressed as follows:

$$P_n(t) = \frac{e^{-\lambda t} (\lambda t)^n}{n!} \tag{3}$$

Where $P_n(t)$, represents the probability of having n incidents in time period of t ; and λ is the mean rate of earthquake occurrence in unit time. So, to predict the earthquake occurrence in Bandar-e-Anzali region, first the Poisson behavior of earthquakes is evaluated.

The earthquake catalog studied in this study, after culling and removal of aftershocks and foreshocks by using time and space windows method, includes 160 earthquakes (Appendix 1). Among the remaining earthquakes of the catalog, excluding the historical earthquakes due to their long-term duration, the instrumental earthquakes (since 1900 to 2013) are grouped in 1-year intervals. Thus, 112-time intervals are resulted through which all numbers of the instrumental earthquakes of the catalog are distributed and tabulated such that the number of earthquakes occurred in each 1-year interval can be observed from the table. The results of this investigation are shown in histogram of Figure-3 where horizontal axis represents the number of earthquakes per intervals and the vertical axis is the number of 1-year intervals. For example, the

number of 1-year intervals through which no earthquake has occurred is 50.

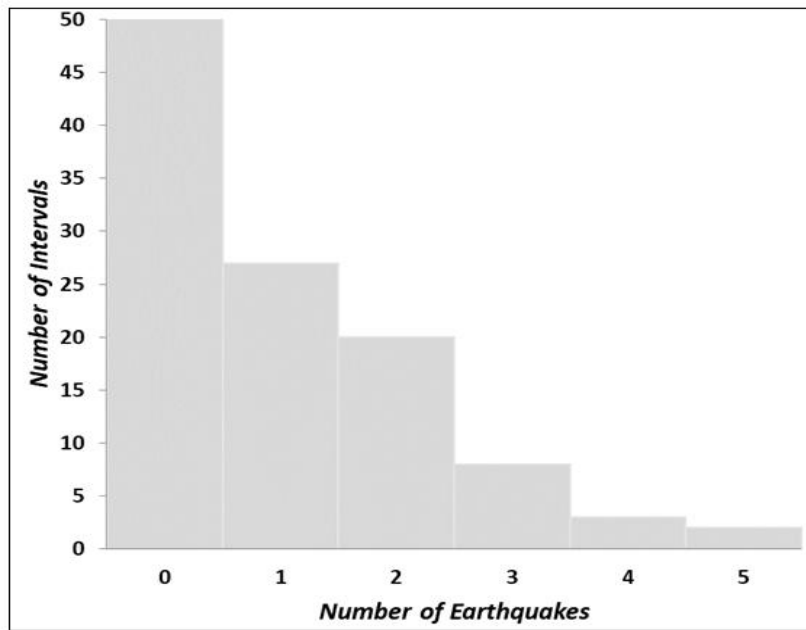


Fig-3: Scatter diagrams of mainshocks for Bandar-e-Anzali with MTL greater than 3.5

By following the above steps, the probability of earthquake occurrence is eventually obtained in time intervals 1, 75, 475 and 2475 years, as well as the return period of the earthquakes with different magnitudes using Kijko method, presented in Table-5. It is

observed that Iranian seismic code 2800 yields the design earthquake with a return period of 475 years slightly greater than 7 in terms of surface-wave scale M_s .

Table-5: The probability of earthquake occurrence in terms of magnitude and the return period for Bandar-e-Anzali area

Earthquake Magnitude (M_s)	Return Period (year)	Probability of Occurrence (%)			
		in one year	in 75 years	in 475 years	in 2475 years
3.5	0.3	98.0	100	100	100
4	0.7	74.0	100	100	100
4.5	2.2	37.1	100	100	100
5	6.3	14.7	100	100	100
5.5	18.3	5.3	98.4	100	100
6	53.2	1.8	75.6	100	100
6.5	155.7	0.6	38.2	95.3	100
7	461.1	0.2	15.0	64.3	99.5
7.5	1414.3	0.07	5.2	28.5	82.6
8	4915.7	0.02	1.5	9.3	39.7

Design Response Spectra

The general form of the attenuation law that has been accepted by many researchers is displayed in the equation (4) [27]:

$$Y = b_1 \cdot f_1(M) \cdot f_2(R) \cdot f_3(M, R) \cdot f_4(P_i) \cdot \varepsilon \quad (4)$$

In this equation, Y is the strong ground motion parameter to be estimated; $f_1(M)$ is a function of magnitude; $f_2(R)$ is a function of distance; $f_3(M, R)$ is a joint function of magnitude and distance; $f_4(P_i)$ is the representative function of the path parameters, conditions of site or constructions; and finally ε is a

random variable to express the uncertainty embedded in Y.

Constants and coefficients of these relationships are obtained by regression analysis of the observational data (in most cases the peak ground acceleration or spectral acceleration values). In many parts of the world, hundreds of attenuation relationships have been introduced, while in many other areas, no attenuation relationship exists for peak ground acceleration or spectral acceleration. The main reason is the lack of genuine database. In Iran, located in a very seismic prone area, despite the existence of one of the largest accelerogram networks of the world and having

a rich accelerograms database, unfortunately few studies have been carried out in this field. Nonetheless, many researchers believe that an identified model for a specific region can be used in areas with similar characteristics [28]. Though, using an attenuation relationship of a specific region in other areas with different shell profile and tectonic is not yet permitted simply without the necessary modifications. Detailed knowledge of the seismotectonic, details of the earthquakes data in the given area including magnitude, epicentral distance, focal depth, location, slope and interfaces of the rupturing fault, its mechanism, and also information on the soil condition of the site are necessary in a study to fit a reliable attenuation relationship [29].

In order to reach a specific relationship for the area under study, most of the attenuation laws, relevant to different parts of Iran, were assessed and evaluated. Finally, three valid and useful attenuation relationships, presented as response spectra for Iran were opted for further investigations.

The first relationship was presented by Ambraseys *et al.*, [30]. Data used in this model is the acceleration maps related to 157 earthquakes around the world, which are mostly related to Northwest America, with the explanation that the records related to the several earthquakes in Iran, such as Naghan, Tabas, and Manjil are also included. Focal depths of the cases used are less than 30 km, with 81 percent of the focal depths lying between 5 km and 15 km.

The next relationship was introduced by Campbell and Bozorgnia [31-33]. Most of the data used in this model, are seismographs related to U.S. state of California. Other data used are related to different parts of the world, including Alaska, Armenia, Canada, Hawaii, India, Iran, Japan, Mexico, Nicaragua, Turkey, and Uzbekistan. It should be noted that the earthquakes used in this context, have focal depths less than 25 km.

The third relationship was presented by Ambraseys and Douglas [34]. Data used in this model is related to seismographs around the world, most of them are related to the Northwest America (133 records, 72%), some are from Europe (40 records, 22%) and the rest is from Japan, Canada, Nicaragua and Taiwan, were all of them are shallow earthquakes with focal depths falling between 1 km and 19 km.

According to the profile mentioned in the estimation of the aforementioned attenuation relationships and due to the fact that most of the earthquakes occurred in Iran, including Bandar-e-Anzali range, are sourced from shallow ground, some of which are utilized in the aforementioned relationships, it is conceived that these relations are presumably useful to assess strong ground motion parameters for the areas in Iran. However, for precise operation of these relationships, they are utilized in a logic tree scheme as illustrated in Figure-4. Obviously, each of the aforesaid relationships is assigned a weight, proportional to their reliability and accuracy.

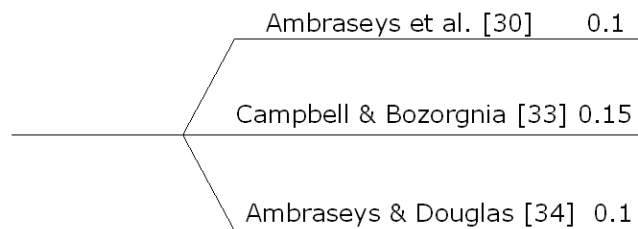


Fig-4: Attenuation relationships considered for estimation of the site-specific response spectra of Bandar-e-Anzali

Thus, the response spectra of horizontal and vertical components of ground acceleration for Bandar-e-Anzali and suburbs are obtained for earthquakes with

occurrence probability of 50% in 50 years, 10% in 50 years, and 2% in 50 years in Figure-5.

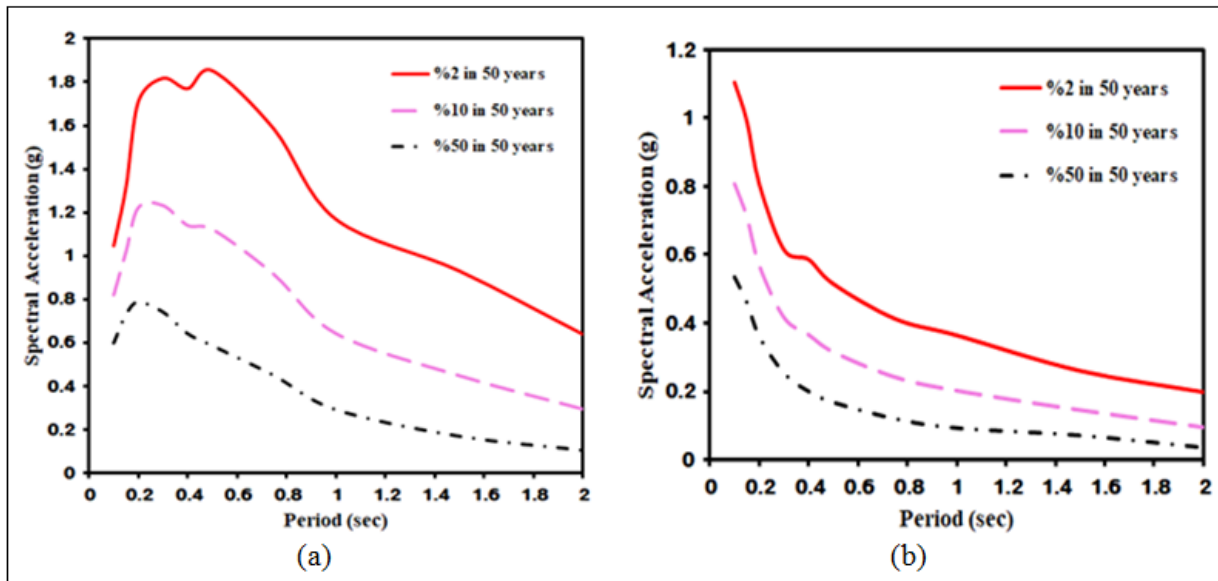


Fig-5: Site specific response spectra for the zone of Bandar-e-Anzali; a) horizontal component; and b) vertical component

Figure-6 also represents the difference between site specific response spectra related to the horizontal and vertical acceleration components of Bandar-e-Anzali and suburbs with occurrence probability of 10% in 50 years according to the Iranian seismic code 2800 design spectrum. Comparison of both illustrations shows that the values of the standard

design spectrum are higher than the vertical acceleration component response spectra in all periods except 0.1 s, however for the horizontal component mixed behavior is observed. The values of the standard design spectrum are less than the horizontal site-specific response spectrum for periods less than 0.9 s. But they become slightly higher afterwards.

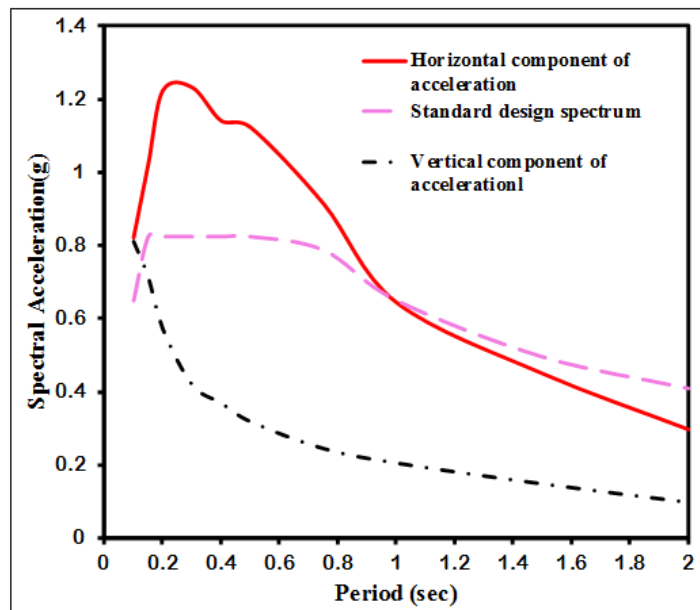


Fig-6: Standard design spectrum in comparison to the site-specific response spectra of Bandar-e-Anzali for occurrence probability of 10% in 50 years

Estimation of Peak Ground Acceleration (PGA)

To estimate the peak ground acceleration in Bandar-e-Anzali zone, SeisRisk III, seismic hazard analysis software was used [35]. Although other software could genuinely be employed for the same purpose, SeisRisk III is usually the researcher's preference for zonation map of the peak ground

acceleration in Iran [20]. Several new and authentic earthquakes occurred in the Bandar-e-Anzali region were used, which are presumed leading to high reliability result. For this purpose, the logic tree approach was used as illustrated in Figure 8. In fact, after assigning a weight to each relationship as shown in Figure 7(a) combination of 8 attenuation

relationships was adopted to render the peak ground acceleration for the desired area. For estimation of the vertical component of the peak ground acceleration, 5 relevant attenuation laws and the logical tree related to these relationships have been shown in Figure 7(b).

Zonation of Peak Ground Acceleration

Using 8 authentic, new and compatible attenuation relationships in Figure-7 by logic tree method for the earthquakes occurred in the Bandar-e-Anzali area, the results of zonation of the horizontal component of the peak ground acceleration from seismic hazard analysis for zone of Bandar-e-Anzali

and suburbs are presented. Indeed, they are estimated for earthquakes to probability occurrence of 50% in 50 years, 10% in 50 years, and 2% in 50 years as illustrated in Figures 8 to 10, respectively.

Furthermore, using five useful, valid, and up to date relationships represented in Figure 7(b), the results of zonation of the vertical component of peak ground acceleration are obtained from seismic hazard analysis for zone of Bandar-e-Anzali and suburbs. These PGAs are estimated for earthquakes with occurrence probability of 50% in 50 years, 10% in 50 years and 2% in 50 years as shown in Figures 11 to 13, respectively.

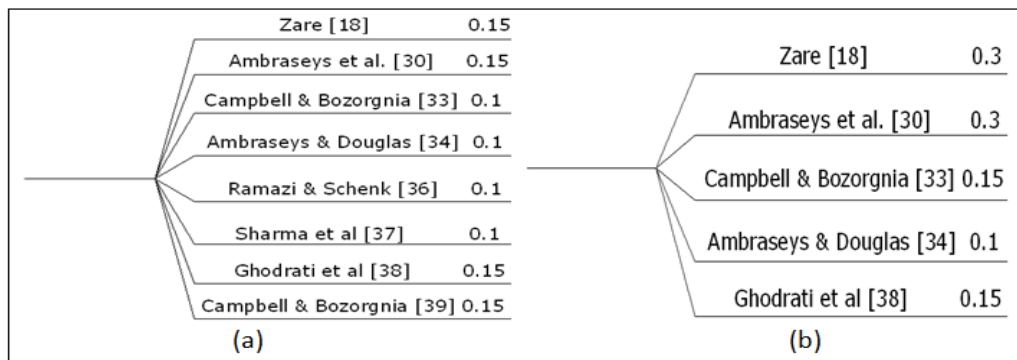


Fig-7: Applied logic tree for seismic hazard analysis; a) horizontal component; b) vertical component

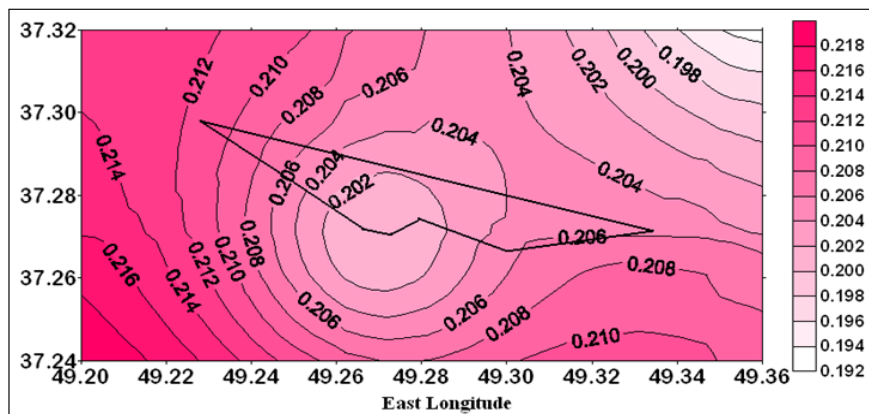


Fig-8: Horizontal seismic hazard (PGA over bedrock) map of Bandar-e-Anzali and suburbs using logic tree for earthquakes with occurrence probability of 50% in 50 years

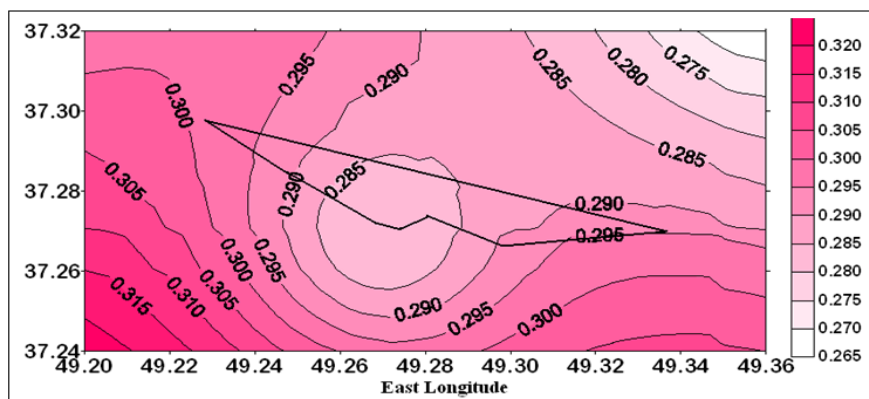


Fig-9: Horizontal seismic hazard (PGA over bedrock) map of Bandar-e-Anzali and suburbs using logic tree for earthquakes with occurrence probability of 10% in 50 years

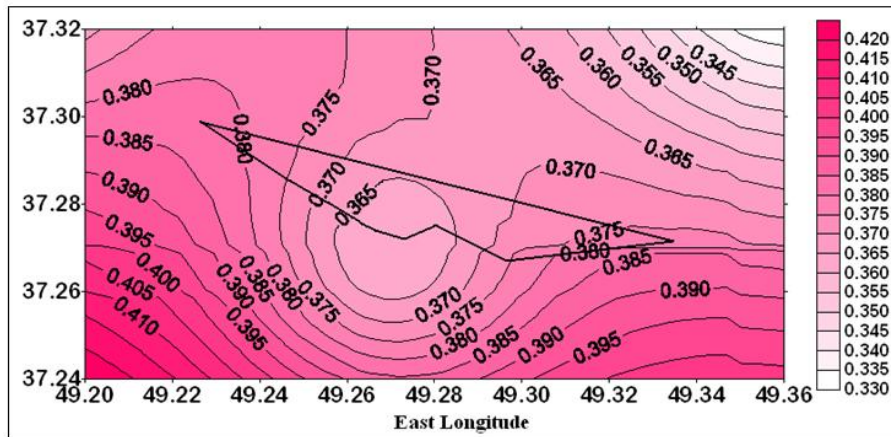


Fig-10: Horizontal seismic hazard (PGA over bedrock) map of Bandar-e-Anzali and suburbs using logic tree for earthquakes with occurrence probability of 2% in 50 years

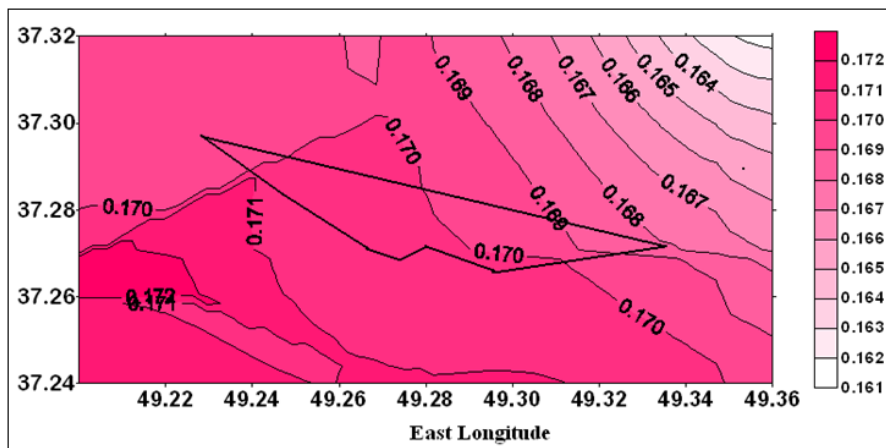


Fig-11: Vertical seismic hazard (PGA over bedrock) map of Bandar-e-Anzali and suburbs using logic tree for earthquakes with occurrence probability of 50% in 50 years

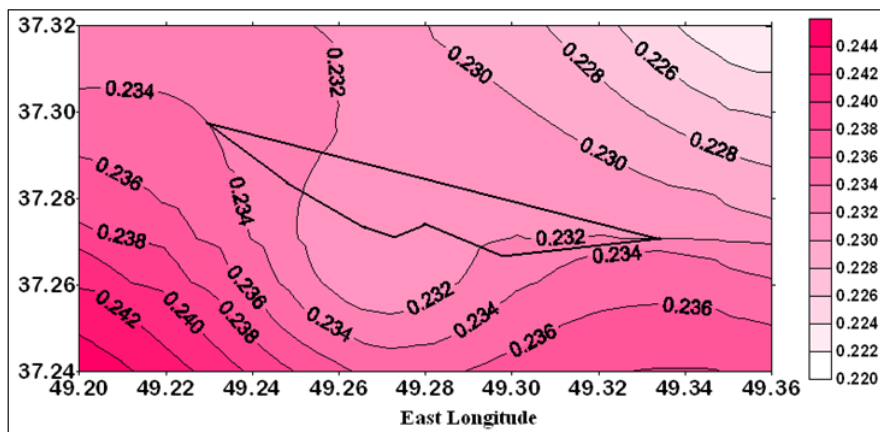


Fig-12: Vertical seismic hazard (PGA over bedrock) map of Bandar-e-Anzali and suburbs using logic tree for earthquakes with occurrence probability of 10% in 50 years

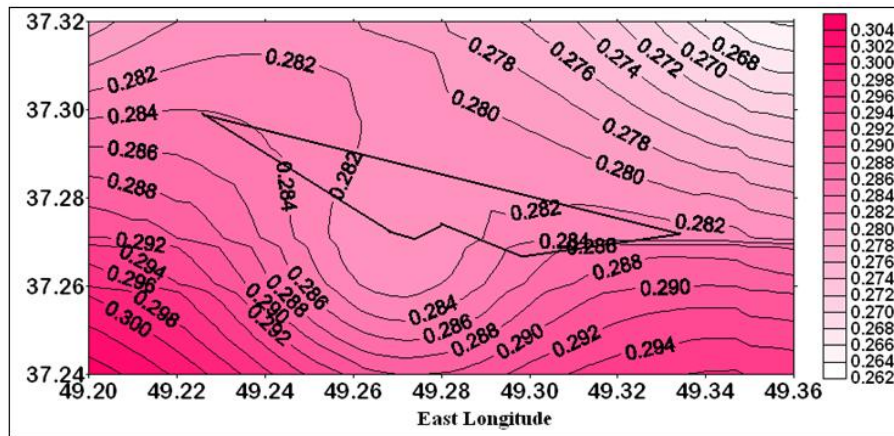


Fig-13: Vertical seismic hazard (PGA over bedrock) map of Bandar-e-Anzali and suburbs using logic tree for earthquakes with occurrence probability of 2% in 50 years

By comparing the values, obtained in this paper for the earthquakes with occurrence probability of 10% in 50 years (457 years return period) and those of local Iranian seismic code 2800, a very good conformity was found. The value of the maximum ground acceleration for Bandar-e-Anzali area is 0.3 in this regulation. It is essential to note that the peak ground acceleration values for both horizontal and vertical components increase from the north to the south, especially to the southeastern and western areas. This increase represents more seismically active parts of the southeastern and western zones as compared to the northern parts of the region. The final remark is that the central part of this range is located in the “Security Pit” and is more secure than other areas.

CONCLUSION

Bandar-e-Anzali is the largest northern Port of Iran with approximately 275 square kilometers and population exceeding 150000. It has always experienced many severe earthquakes due to the proximity to many active faults. The main aim of the present investigation is estimating the peak ground horizontal and vertical acceleration components of earthquake in the zone of Bandar-e-Anzali. To this end, the last status of major faults with historical reports and instrumental records of earthquakes until the end of 2013 A.D., occurred within 200 km radius of Bandar-e-Anzali, was collected and studied.

In this paper, after culling and removal of the aftershocks and the foreshocks by time and space windows method, Poisson behavior of the remaining earthquakes was studied. Then by calculating the frequency of earthquakes and using seismic hazard analysis of Kijko 2000 computer program, in the first step, seismicity parameters and in the next steps site specific response spectra and zonation of the peak ground accelerations have been assessed for Bandar-e-Anzali and suburbs.

By precise look in the seismicity parameters obtained from combination of historical and instrumental data, it is observed that in estimating seismic coefficients, the historical earthquakes have enjoyed greater participation percentage (about 34%), but to get the average rate of earthquakes (λ_m), the second type of instrumental data (1964-2003) had contributed more (about 45%). The rationale behind these results are the short-time period instrumental earthquakes recorded, considerable historical earthquake magnitude reported, and also the greater number of the second type instrumental data (about 65 data) earthquakes in the catalog of Bandar-e-Anzali zone.

Investigation of the Poisson behavior of earthquakes shows that due to a good alignment of the data to the Poisson model, calculations performed by Kijko method, gives the correct answer. According to the responses obtained from this method, the possibility of an earthquake with high intensity and short return period is not unexpected and needs special attention. However, by comparing them with previous results, it appears that the time periods of the data, will have many impacts on the results, therefore it is better to inspect the probability of the occurrence of earthquakes in the region every few years.

The values of peak ground acceleration zoned in this range, indicate that they increase for both horizontal and vertical components, from north to south, especially to the southeastern and western regions. This increase represents that southeastern and western areas are more prone to earthquake as compared to northern parts. The central part of this range is marked as the “Security Pit” and is more secure towards the eastern and western and southern areas.

Disclosure

No funding was used for the current study and no conflict of interests is concerned.

Appendix 1

Table A-1: Catalog of the main shocks with magnitudes greater than 4 on the surface-wave magnitude scale in Iran

No.	Origin Time		Epicenter		FD	Magnitude			Ref.	Dist.
	D-M-Y	h:m:s	lat.	lon.		m _b	M _S	M _L		
1	0/1/864		35.7	51			5.3		AMB	241
2	23/2/958		36	51.1			7.7		AMB	221
3	12/10/1119		35.7	49.9			6.5		AMB	202
4	0/5/1177		35.7	50.7			7.2		AMB	227
5	8/15/1485	6:00:00	36.7	50.5			7.2		AMB	127
6	0/0/1593		37.8	47.5			6.1		AMB	181
7	4/20/1608	12:00:00	36.4	50.5			7.6		AMB	152
8	2/3/1678	6:00:00	37.2	50			6.5		AMB	57
9	12/16/1808	18:00:00	36.4	50.3			5.9		AMB	141
10	5/19/1844	19:00:00	37.4	48			6.9		AMB	132
11	10/1/1854	15:00:00	38	50			5.9		AMB	76
12	12/30/1863	22:00:00	38.2	48.6			6.1		AMB	113
13	10/20/1876	15:00:00	35.8	49.8			5.7		AMB	189
14	3/22/1879	4:00:00	37.8	47.9			6.7		AMB	146
15	7/4/1880		36.5	47.5			5.6		AMB	208
16	5/3/1883	12:00:00	37.9	47.2			6.2		AMB	210
17	1/4/1896	16:00:00	37.8	48.4			6.7		AMB	103
18	5/20/1901	12:29:00	36.39	50.48			5.4		AMB	151
19	2/9/1903	5:18:00	36.58	47.65			5.7		AMB	192
20	6/24/1903	16:56:00	37.48	48.96			5.9		AMB	46
21	1/9/1905	6:17:00	37	48.68			6.2		AMB	88
22	3/20/1906	23:45:00	38.9	49	15		4.3		MOS	165
23	12/4/1910	14:02:00	38.8	48.8	33		5.1		KAR	160
24	4/16/1913	6:00:00	38.7	48.5	33		5.2		KAR	162
25	9/24/1913	16:05:00	38.5	48.9	18		4.2		MOS	126
26	6/2/1917	0:28:12	38	48.5		5			NOW	105
27	2/19/1924	7:01:00	39	48.32		6.8			AMB	199
28	10/31/1927	6:23:00	36.5	49			4		NOW	117
29	3/24/1928	10:53:29	38.14	48.17	18	5			NOW	139
30	3/28/1928	19:43:00	38.7	49	10		4.2		MOS	143
31	8/28/1929	19:43:00	38.7	49	10		4.2		MOS	143
32	3/2/1932	9:00:37	38.5	48.3			4		MOS	156
33	5/24/1932	23:31:55	39.33	48.6			4.5		NOW	222
34	4/16/1933	6:54:45	38.82	48.34	146		4.8		NOW	182
35	11/9/1944	19:39:40	38	48.4			4.2		KAR	113
36	6/17/1948	14:08:31	36.5	49		5.2			ISS	117
37	6/30/1948	19:31:50	36.66	49.48	114			5	NOW	91
38	6/18/1949	1:14:04	38.7	49	10		4		MOS	143
39	5/27/1950	7:03:00	39	48.6			4		NAB	188
40	1/16/1951	17:53:52	39.31	49.6	5	5			NOW	206
41	6/5/1951	3:34:59	36.18	48.33	81		4.6		NOW	177
42	7/18/1952	0:43:51	37.5	50.1		4.7			ISS	57
43	5/10/1955	11:32:28	38.6	48			4		MOS	182
44	4/12/1956	22:34:49	37.3	50.2	30	5.5			ISS	69
45	4/13/1956	9:38:14	38.5	48.4			4		TUC	150
No.	Origin Time		Epicenter		FD	Magnitude			Ref.	Dist.
	Y-M-D	h:m:s	lat.	lon.		m _b	M _S	M _L		
46	8/19/1957	7:22:19	37.49	49.71		4.5			NOW	22
47	7/6/1958	10:46:01	38.5	48.4	14		4		MOS	150
48	5/1/1959	8:24:03	36.45	51.23	44	5.7			ISS	195
49	5/31/1959	13:01:44	37.67	48.94		5			NOW	52
50	7/31/1959	10:28:06	38.86	49.38	35	4.8			NOW	155

51	11/25/1959	0:58:00	38.5	50.3			4.2		CCP(BAN)	137
52	6/23/1960	3:37:42	37	49.5				6.5	FS	53
53	9/1/1962	19:20:00	35.71	49.81	21		7.2		AMB	199
54	11/24/1962	14:14:26	38.5	47.7		4.5			NOW	196
55	11/25/1962	0:07:07	38.8	48.4		4.5			NOW	177
56	2/8/1964	6:28:23	37.07	50.99	11	4.6			NOW	144
57	3/29/1964	23:03:43	39.2	49	14		4.6		MOS	197
58	11/4/1964	4:27:14	38.7	49.3	20		4		MOS	138
59	10/29/1965	15:59:42	37.9	48.7	33	4.6			USCGS	84
60	9/30/1966	15:17:33	38.3	48			4		ZEM	161
61	11/8/1966	3:14:14	36.1	50.8	38	5			USGS	195
62	7/11/1967	1:25:50	38.2	47.8	20		4.3		MOS	171
63	8/25/1967	12:26:46	35.56	49.24	8	4.7			EHB	215
64	6/4/1968	1:44:25	37.5	49.19	49	4.6			ISC	25
65	8/2/1968	3:59:27	36.85	49.33	36	4.7			ISC	71
66	4/16/1970	1:26:50	38.81	48.61	30	4.6			EHB	168
67	7/11/1970	22:41:13	37.54	49.03	20	5.2			EHB	40
68	5/15/1971	4:53:07	37.96	49.04	50	4.7			ISC	67
69	1/18/1972	21:12:01	37.5	48.84	10	4.8			EHB	57
70	6/13/1973	10:05:26	38.46	49.52	48	4.5			ISC	110
71	9/17/1973	4:06:04	36.52	51.11	47	4.8			USGS	182
72	4/11/1975	14:26:44	35.55	50.17	50	4.7			USGS	224
73	5/26/1978	13:42:01	37	50			6.3		HFS1	71
74	11/3/1978	18:52:59	37	51		5			HFS	148
75	11/4/1978	15:22:20	37.67	48.91	34	6	6.1		EHB	55
76	11/8/1979	5:21:59	38.74	48.84	33	4.7			USGS	152
77	2/19/1980	1:06:05	39.13	48.79	43	4.9			ISC	195
78	5/5/1980	10:21:48	38.08	49.01	33	4.6			USGS	79
79	7/22/1980	5:17:08	37.32	50.26	62	5.3	5.1		EHB	73
80	8/4/1981	18:35:43	38.15	49.38	25.7	5.4	5.2		EHB	76
81	8/4/1981	18:53:59	36.45	51.27		4.7			ISC	198
82	10/30/1981	10:54:16	38.91	49.86		4.6			ISC	164
83	4/2/1983	0:32:28	38.98	48.7	15	4.7			EHB	182
84	7/22/1983	2:40:59	36.94	49.22	41	5.6	5		EHB	64
85	12/20/1983	22:21:05	36.8	50.79	42	4.8			USGS	141
86	9/9/1984	17:54:59	35.58	49.34	33	4.6			USGS	212
87	9/30/1984	15:33:21	37.92	49.16	59	4.6			ISC	57
88	4/3/1985	1:44:26	38.1	48.42	26	4.7			USGS	117
89	11/2/1985	9:34:14	37.52	49.07	33	4.5			USGS	36
90	1/27/1986	16:35:50	38.92	48.71	71	5.3	4.3		EHB	175
91	4/29/1986	22:07:56	37.9	49.11	25	4.9			EHB	58
92	8/28/1986	7:49:10	39.51	49.27	33	4.5			ISC	228
93	11/5/1986	1:15:39	38.69	48.62	86	4.5			USGS	156
94	1/14/1988	11:29:20	36.01	50.6	33	4.6			USGS	193
95	2/15/1989	10:10:08	37.29	50.3	53	4.7			EHB	78
No.	Origin Time		Epicenter		FD	Magnitude			Ref.	Dist.
	Y-M-D	h:m:s	lat.	lon.		m _b	M _S	M _L		
96	10/8/1989	14:13:29	37.04	50.12	57	4.6			USGS	76
97	6/20/1990	21:00:13	37	49.22	19	6.2	7.4		EHB	57
98	6/20/1990	23:27:47	36.65	50.05	15	4.6	5		EHB	106
99	9/24/1990	6:35:14	38.16	48.15	10	4.6			ISC	141
100	4/8/1993	9:48:03	37.9	47.99	10	4.7			USGS	141
101	11/2/1994	12:31:01	38.15	48.31	10	5			USGS	129
102	12/3/1994	1:35:51	37.64	49.35	33	4.8			USGS	21
103	4/26/1995	11:46:12	36.93	49.4	33	4.6	4.2		EHB	61
104	5/15/1995	0:16:54	38.49	49.43	26	4.7	4.2		EHB	114
105	5/27/1995	21:21:32	39.03	48.94	33	4.8			USGS	180
106	6/26/1995	21:12:54	36.6	51.19	21.9	4.1	4.2		ISC	183

107	10/15/1995	6:56:35	37.03	49.47	25	4.9			EHB	49
108	1/3/1996	8:42:24	38.95	48.73	35	4.9			EHB	178
109	2/28/1997	12:57:20	38.12	48.08	9.7	5.5	6.1		EHB	144
110	6/7/1997	20:29:48	36.51	50.36	33	3.9	4.2		ISC	134
111	2/28/1998	0:39:10	36.99	48.76	52	4.5	4.1		EHB	83
112	4/4/1998	2:46:33	36.65	49.43	33	4.5			USGS	92
113	7/9/1998	14:19:20	38.73	48.53	26	5.8	5.5		EHB	164
114	9/28/1998	17:26:30	36.58	48.75	47	4.7			USGS	119
115	12/3/1998	13:13:33	36.05	50.88	33	4.5			USGS	204
116	10/29/2001	10:04:49	38.92	48.64	53	4.6			USGS	178
117	1/5/2002	14:43:42	37.52	49.02	21	4.5			USGS	41
118	2/14/2002	20:06:23	36.9	49.4	49	4.5			USGS	64
119	4/19/2002	13:46:49	36.51	49.77	12.7	5.2	4.6		EHB	111
120	6/22/2002	2:58:23	35.59	49.03	11	6.2	6.4		EHB	214
121	5/28/2004	17:34:49	36.48	51.36	10	3.7	4		EHB	203
123	8/21/2004	13:53:18	35.43	49.46	10	4.5			USGS	228
124	10/17/2004	21:31:07	35.61	49.15	21	4.6			USGS	210
125	11/8/2004	20:03:20	35.59	49.01	10	4.4		4.6	USGS	214
126	4/11/2005	14:50:31	39.51	49.19	27	4.5			USGS	229
127	5/26/2005	1:59:11	38.81	48.71	75	4.4		4.4	USGS	164
128	9/26/2005	18:57:05	37.29	47.69	15	5	4.2	4.8	EHB	161
129	11/5/2006	20:06:42	37.5	48.9	23.4	4.7	4	5	EHB	51
130	7/11/2007	6:51:15	38.82	48.64	28.6	4.9	4.2	4.9	ISC	168
131	12/14/2007	21:56:04	37.27	47.7	32	4.6	3.3	4.4	USGS	161
132	3/23/2008	12:11:31	37.31	48.51	6	4.8	3.8	4.7	USGS	88
133	3/27/2008	6:48:57	35.78	49.94	2			4	ISC	196
134	5/27/2008	6:18:08	36.65	48.66	23	4.9		5.4	USGS	117
135	9/26/2008	11:00:06	35.56	48.91	10	4.3		4.3	USGS	220
136	10/22/2010	8:00:38	37.96	49.09	15			4.6	IIEES	64
137	3/4/2011	9:46:29	37.73	48.61				4.3	IIEES	82
138	2/4/2012	20:04:14	37.7	49.53	14			4.5	IIEES	26
139	3/18/2012	2:38:16	36.82	49.2	14			4.5	IIEES	77
140	7/6/2013	17:07:50	37.52	48.72	6			4.3	IIEES	68
141	11/8/2013	10:12:35	37.86	47.27	15			4.5	IIEES	202.49

References of the Catalogue:	
A28	Ambraseys and Melville,1982 and Ambraseys,1988
AMB	Ambraseys,N.N,Melville,C.P.,1982
AMB88	Ambraseys,1988
BAN	Banisadr,M.,1969
BCIS,BCI	Bureau Central International de Seismologie,Strasbourg,France
BE	Bob Engdahl
BER,M	Berberian,Geological and Mining Survey of Iran
Ber77	Berberian,1977
BS	BCIS
C69	Canitez,1969
CCP	Atlas USSR earthquake
CGS	U.S. Coast and Geodetic Survey,USA
CH81	Chandra,1981
CP	USSR station bulletins
FS	Fisher
IGTU	Institute of Geophysics University of Tehran
IIEES	International Institute of Earthquake Engineering and Seismology
INSN	Iranian National Broadband Seismic Network
ISC	International Seismological Centre,UK
ISS	International Seismological Summary,UK
KAR	Karnik,1969
KAR.N	"Seismicity of the European Area".D.Riedel Publishing Company Dordrecht,Holland

KSA	Ksara Seismological Observatory Lebanon
MEA	Riad and Meyers,1985
MOS	Moscow,U.S.S.R.
NAB	Nabavi,Institute of Geophysics-Tehran University
NOW	Nowroozi
PT	Publications of Institute of Geophysics-Tehran University
QJA	Quitmeyer and Jacob,1979
RU	Rustanovic
SHI,SHR	Shiraz
SSK	Savarenskii et al.,eds.1962,Atlas zemletrissenii v S.S.S.R
STR	Strasbourg,France
TUC	Tucson,Arizona,USA
ULM	Catalog of earthquakes compiled by V.I. Ulomov;Russian Academy of Sciences,Moscow
USCGS	United States Coast and Geodetic Survey
USGS	United States Geological Survey
ZEM	Zemletrayaseviyi V SSSR,Moscow

REFERENCES

- Berberian, M. (1981). Active faulting and tectonics of Iran. *Zagros-Hindu Kush-Himalaya Geodynamic Evolution*, 3, 33-69.
- Berberian, M., Qorashi, M., Jackson, J. A., Priestley, K., & Wallace, T. (1992). The Rudbar-Tarom earthquake of 20 June 1990 in NW Persia: preliminary field and seismological observations, and its tectonic significance. *Bulletin of the Seismological Society of America*, 82(4), 1726-1755.
- Alavi, M. (1996). Tectonostratigraphic synthesis and structural style of the Alborz mountain system in northern Iran. *Journal of Geodynamics*, 21(1), 1-33.
- Berberian, M., & Yeats, R. S. (2001). Contribution of archaeological data to studies of earthquake history in the Iranian Plateau. *Journal of Structural Geology*, 23(2-3), 563-584.
- Jackson, J., Priestley, K., Allen, M., & Berberian, M. (2002). Active tectonics of the south Caspian basin. *Geophysical Journal International*, 148(2), 214-245.
- Zare, M., Ghafory-Ashtiany, M., & Bard, P. Y. (1999). Attenuation law for the strong-motions in Iran. In *Proceedings of the third international conference on seismology and earthquake engineering* (Vol. 1, pp. 345-354).
- International Institute of Earthquake Engineering and Seismology, Internet Website: <http://iiees.ac.ir>.
- Ambraseys, N. N., & Melville, C. P. (2005). *A history of Persian earthquakes*. Cambridge university press.
- Gardner, J. K., & Knopoff, L. (1974). Is the sequence of earthquakes in Southern California, with aftershocks removed, Poissonian?. *Bulletin of the Seismological Society of America*, 64(5), 1363-1367.
- Kijko, A., & Sellevoll, M. A. (1989). Estimation of earthquake hazard parameters from incomplete data files. Part I. Utilization of extreme and complete catalogs with different threshold magnitudes. *Bulletin of the Seismological Society of America*, 79(3), 645-654.
- Kijko, A., & Sellevoll, M. A. (1992). Estimation of earthquake hazard parameters from incomplete data files. Part II. Incorporation of magnitude heterogeneity. *Bulletin of Seismological Society of America*, 82(1), 120-134.
- Kijko, A. (2000, May). Statistical estimation of maximum regional earthquake magnitude M_{max} . In *Workshop of Seismicity Modeling in Seismic Hazard Mapping, Poljce, Slovenia, Geological Survey* (pp. 1-10).
- Nowroozi, A. A. (1985). Empirical relations between magnitudes and fault parameters for earthquakes in Iran. *Bulletin of the Seismological Society of America*, 75(5), 1327-1338.
- Mirzaei, N. (2002). Basic parameters of earthquakes in Iran. *Geophysics Institute of Tehran University*. 1-295.
- Nowroozi, A. A., & Ahmadi, G. (1986). Analysis of earthquake risk in Iran based on seismotectonic provinces. *Tectonophysics*, 122(1-2), 89-114.
- Tavakoli, B., & Ghafory-Ashtiany, M. (1999). Seismic hazard assessment of Iran. *Annali di Geofisika*, 42(6), 1013-1021.
- Amiri, G. G., Khorasani, M., Hessabi, R. M., & Amrei, S. R. (2009). Ground-motion prediction equations of spectral ordinates and Arias intensity for Iran. *Journal of Earthquake Engineering*, 14(1), 1-29.
- Hamzehloo, H., Alikhanzadeh, A., Rahmani, M., & Ansari, A. (2012). Seismic hazard maps of Iran. In *Proceedings of the 15th World Conference on Earthquake Engineering, Lisbon, Portugal* (pp. 24-28).
- Zare, M. (2017). Seismic Hazard Zoning in Iran: A State-of-the-Art on the Studies during Four Decades. *Journal of Seismology & Earthquake Engineering*, 19(2) 71-101..
- Ghodrati, A. G., Motamed, R., & Rabet Es-Haghi, H. (2003). Seismic hazard assessment of

- metropolitan Tehran, Iran. *Journal of Earthquake Engineering*, 7(3), 347-372.
21. Ghodrati Amiri, G., & Amrei, S. R. (2008). Seismic hazard assessment of Gilan province including Manjil in Iran. In *The 14th World Conference on Earthquake Engineering, Beijing, China*.
 22. Ghodrati, A., Andisheh, K., Razavian, A., & Seyed, A. (2009). Probabilistic seismic hazard assessment of Sanandaj, Iran. *Structural Engineering and Mechanics*, 32(4), 563-581.
 23. Moghaddam, H., Fanaie, N., & Hamzehloo, H. (2009). Uniform hazard response spectra and ground motions for Tabriz. *Journal of Scientia Iranica*, 16(3), 238-248.
 24. Alizadeh, B. P. S. & Jamshidi, R. C. (2011). Introduction Valid Correlation between the Earthquake Magnitude Scales in Iran. In *6th National Congress of Civil Engineering, Semnan University, Semnan, Iran, (in Persian)*.
 25. Gutenberg, B., & Richter, C. F. (1955). Seismicity of the Earth and Associated Phenomena. Eleventh Edition. *Published by Sagwan Press*.
 26. Alizadeh, B. (2011). *Earthquake Hazard Analysis to Determine the Peak Ground Acceleration in Bandar-e-Anzali City and Its Suburbs* (Doctoral dissertation, M. Sc. Thesis, University of Guilan, Rasht, Iran, (in Persian)).
 27. Kramer, S. L. (1996). Geotechnical earthquake engineering. In *prentice-Hall international series in civil engineering and engineering mechanics. Prentice-Hall, New Jersey*.
 28. Fukushima, Y., Berge-Thierry, C., Volant, P., Griot-Pommer, D. A., & Cotton, F. (2003). Attenuation relation for West Eurasia determined with recent near-fault records from California, Japan and Turkey. *Journal of Earthquake Engineering*, 7(4), 573-598.
 29. Zare, M. (2010). Principles of Earthquake Hazard Analysis. *International Institute of Earthquake Engineering and Seismology Press*.
 30. Ambraseys, N. N., Simpson, K. U., & Bommer, J. J. (1996). Prediction of horizontal response spectra in Europe. *Earthquake Engineering & Structural Dynamics*, 25(4), 371-400.
 31. Campbell, K. W., & Bozorgnia, Y. (2003). Updated near-source ground motion relations for the horizontal and vertical components of peak ground acceleration and acceleration response spectra. *Bulletin of the Seismological Society of America*, 93(3), 1413.
 32. Campbell, K. W., & Bozorgnia, Y. (2003). Updated near-source ground motion relations for the horizontal and vertical components of peak ground acceleration and acceleration response spectra. *Bulletin of the Seismological Society of America*, 93(4), 1872.
 33. Campbell, K. W., & Bozorgnia, Y. (2004). Updated Near-Source Ground Motion Relations for the Horizontal and Vertical Components of Peak Ground Acceleration and Acceleration Response Spectra. *Bulletin of the Seismological Society of America*, 93(1), 314-331.
 34. Ambraseys, N. N., & Douglas, J. (2003). Near-field horizontal and vertical earthquake ground motions. *Soil dynamics and earthquake engineering*, 23(1), 1-18.
 35. Bender, B., & Perkins, D. M. (1987). *SEISRISK III: a computer program for seismic hazard estimation* (No. 1772). US Government Printing Office.
 36. Ramazi, H. R., & Schenk, V. (1994). Preliminary results obtained from strong ground motion analyses of Iranian earthquakes. *Proceedings, XXIV General Assembly of the ESC*, 3, 1762-1770.
 37. Sharma, M. L., Douglas, J., Bungum, H., & Kotadia, J. (2009). Ground-motion prediction equations based on data from the Himalayan and Zagros regions. *Journal of Earthquake Engineering*, 13(8), 1191-1210.
 38. Amiri, G. G., Mahdavian, A., & Dana, F. M. (2007). Attenuation relationships for Iran. *Journal of Earthquake Engineering*, 11(4), 469-492.
 39. Campbell, K. W., & Bozorgnia, Y. (2014). NGA-West2 ground motion model for the average horizontal components of PGA, PGV, and 5% damped linear acceleration response spectra. *Earthquake Spectra*, 30(3), 1087-1115.